Since January 2020 Elsevier has created a COVID-19 resource centre with free information in English and Mandarin on the novel coronavirus COVID-19. The COVID-19 resource centre is hosted on Elsevier Connect, the company's public news and information website.

MAYO CLINIC

ORIGINAL ARTICLE

Acute Kidney Injury in Severe COVID-19 Has Similarities to Sepsis-Associated Kidney Injury: A Multi-Omics Study

Mariam P. Alexander, MD; Kiran K. Mangalaparthi, PhD; Anil K. Madugundu, MTech; Ann M. Moyer, MD, PhD; Benjamin A. Adam, MD; Michael Mengel, MD; Smrita Singh, MBBS; Sandra M. Herrmann, MD; Andrew D. Rule, MD; E. Heidi Cheek, MHS; Loren P. Herrera Hernandez, MD; Rondell P. Graham, MBBS; Denic Aleksandar, MD, PhD; Marie-Christine Aubry, MD; Anja C. Roden, MD; Catherine E. Hagen, MD; Reade A. Quinton, MD; Melanie C. Bois, MD; Peter T. Lin, MD; Joseph J. Maleszewski, MD; Lynn D. Cornell, MD; Sanjeev Sethi, MD; Kevin D. Pavelko, PhD; Jon Charlesworth, MA; Ramya Narasimhan, MBBS; Christopher P. Larsen, MD; Stacey A. Rizza, MD; Samih H. Nasr, MD; Joseph P. Grande, MD; Trevor D. McKee, PhD; Andrew D. Badley, MD; Akhilesh Pandey, MD, PhD; and Timucin Taner, MD, PhD

Abstract

Objective: To compare coronavirus disease 2019 (COVID-19) acute kidney injury (AKI) to sepsis-AKI (S-AKI). The morphology and transcriptomic and proteomic characteristics of autopsy kidneys were analyzed.

Patients and Methods: Individuals 18 years of age and older who died from COVID-19 and had an autopsy performed at Mayo Clinic between April 2020 to October 2020 were included. Morphological evaluation of the kidneys of 17 individuals with COVID-19 was performed. In a subset of seven COVID-19 cases with postmortem interval of less than or equal to 20 hours, ultrastructural and molecular characteristics (targeted transcriptome and proteomics analyses of tubulointerstitium) were evaluated. Molecular characteristics were compared with archived cases of S-AKI and nonsepsis causes of AKI.

Results: The spectrum of COVID-19 renal pathology included macrophage-dominant microvascular inflammation (glomerulitis and peritubular capillaritis), vascular dysfunction (peritubular capillary congestion and endothelial injury), and tubular injury with ultrastructural evidence of mitochondrial damage. Investigation of the spatial architecture using a novel imaging mass cytometry revealed enrichment of $CD3^{+}CD4^{+}$ T cells in close proximity to antigen-presenting cells, and macrophage-enriched glomerular and interstitial infiltrates, suggesting an innate and adaptive immune tissue response. Coronavirus disease 2019 AKI and S-AKI, as compared to nonseptic AKI, had an enrichment of transcriptional pathways involved in inflammation (apoptosis, autophagy, major histocompatibility complex class I and II, and type 1 T helper cell differentiation). Proteomic pathway analysis showed that COVID-19 AKI and to a lesser extent S-AKI were enriched in necroptosis and sirtuin-signaling pathways, both involved in regulatory response to inflammation. Upregulation of the ceramide-signaling pathway and downregulation of oxidative phosphorylation in COVID-19 AKI were noted.

Conclusion: This data highlights the similarities between S-AKI and COVID-19 AKI and suggests that mitochondrial dysfunction may play a pivotal role in COVID-19 AKI. This data may allow the development of novel diagnostic and therapeutic targets.

From the Department of Laboratory Medicine and Pathology (M.P.A., K.K.M., A.K.M., A.M.M., S.S., E.H.C., L.P.P.H., R.P.G., D.A., M.-C.A., A.C.R., C.E.H., R.A.Q., M.C.B., P.T. L., J.J.M., L.D.C., S.S., S.H.N., J.P.G., A.P.), Division of Nephrology and Hypertension (S.M.H., A.D.R., D.A.), Immune Monitoring Core (K.D.P.), Microscopy and Cell Analysis Core (J.C.), Department of Endocrinology (R.N.), Division of Infectious Diseases, Department of Internal Medicine (S.A.R., A.D.B.), Department of Molecular Medicine (A.D.B.), Center for Individualized Medicine (A.P.), Department of Surgery (T.T.), and the Department of Immunology (T.T.), Mayo Clinic, Rochester, MN, USA; Institute of Bioinformatics, International Technology Park, Karnataka, India (K.K.M., A.K.M., S.S.); Amrita School of Biotechnology, Kerala, India (K.K.M.); Manipal Academy of Higher Education, Manipal, Karnataka, India (A.K.M., S.S.); Center for Molecular Medicine, National Institute of Mental Health and Neurosciences, Karnataka, India (A.K.M., S.S., A.P.); Department of Laboratory Medicine and Pathology, University of Alberta, Edmonton, Alberta, Canada (B.A.A., M.M.); Nephropathology Associates, Little Rock, AR, USA (C.P.L.); and the STTARR Innovation Core Facility, University Health Network, Toronto, Ontario, Canada (T.D.M.).

Infection with severe acute respiratory syndrome coronavirus 2 (SARS-CoV-2) causes coronavirus disease 2019 (COVID-19), and is associated with acute kidney injury (AKI) in more than one-third of hospitalized patients.[1] The AKI is often moderate to severe, and is an independent risk factor for in-hospital mortality.[2,3] Acute tubular injury is considered the pathological hallmark of COVID-19 kidney disease as shown in both native and autopsy renal studies.[4-6] Microthrombi, described in heart and lungs,[7-11] is infrequently reported in kidneys.[5,12] Similarly, although severe COVID-19 is associated with a systemic inflammatory response and inflammation in both lungs and heart, little is known about the immune response in the kidneys.

Direct viral toxicity, hemodynamic instability, cytokine storm, and immune-mediated injury have all been proposed as likely causes of renal injury in COVID-19.[5,13,14] Recent studies have drawn similarities between sepsis-associated AKI (S-AKI) and COVID-19–related kidney injury.[15,16] To date, reports evaluating the renal pathology in COVID-19 have largely focused on light microscopy and ultrastructural studies; molecular studies have been limited.

Herein, we present a series of COVID-19 patients who underwent postmortem examination with emphasis on renal pathology findings. Our study sought to describe the pathological spectrum of COVID-19–associated renal injury, and to characterize the molecular profile of COVID-19–associated AKI as compared with S-AKI and nonsepsis-related AKI (NS-AKI) to elucidate similarities and differences in underlying pathophysiology.

PATIENTS AND METHODS

Clinical Data

All cases of COVID-19 (as confirmed by antemortem SARS-CoV-2 nasopharyngeal or oropharyngeal polymerase chain reaction) undergoing research-consented postmortem examination at Mayo Clinic (Rochester, MN) between April 2 and September 9, 2020, were included in the study. Salient information for all cases was abstracted from the electronic medical record, including demographic information, disease history (if available), and the presence or absence of chronic underlying conditions.

Two autopsy-derived control cohorts with AKI were selected for comparative purposes: those who died of bronchopneumonia-associated sepsis (S-AKI, n=7) and those who died with AKI not secondary to sepsis or COVID-19 (NS-AKI, n=7).

The study was approved by and conducted according to the requirements of the Institutional Review Board at Mayo Clinic.

Morphological Analyses

A detailed light microscopic evaluation of all 17 autopsies was performed by two renal pathologists (M.P.A. and L.P.H.). Tissue sections were stained with hematoxylin and eosin, periodic acid-Schiff, trichrome, and Jones methenamine silver stains. In addition, immunohistochemical (IHC) evaluation with CD68, CD3, and CD20 to evaluate macrophages, T cells, and B cells was performed in all 17 autopsies. Detailed methods are provided in the Supplemental Appendix (available online at http://www.mayoclinicproceedings.org). Light microscopy analysis was also performed in the two control cohorts.

In a subset of seven COVID-19 cases that had postmortem interval of <20 hours and only mild autolysis, ultrastructural studies, IHC evaluation for SARS-CoV-2 antigens, and in situ hybridization for viral RNA were also performed.

A high-parameter image mass cytometry using 23 different molecular markers was performed on the COVID-19 cases. The detailed methods, including the markers, are provided in the Supplemental Appendix.

Molecular Analyses

Tissue from the well-preserved seven renal autopsy blocks from COVID-19 cases, as well as the two control groups (n=7 each) were analyzed by NanoString platform using the nCounter Human Organ Transplant Panel that profiles expression of 770 genes associated with different pathways related to immune response and tissue injury. Proteomics of the seven cases each in three groups was

performed following laser capture microdissection of the tubulointerstitial compartment excluding any glomeruli and or regions of interstitial fibrosis or tubular atrophy. Apoptosis in each group was assessed by terminal deoxynucleotidyl transferase of dUTP nick end labeling assay.

Statistical Analysis

Postnormalization gene expression analysis was performed using R version 3.6.3 (R Foundation for Statistical Computing, Vienna, Austria). Functional annotation gene sets were derived using NanoString-provided, literature-based annotations.[17,18] Functional annotation gene set expression was determined using the z scores of the mean normalized counts of the constituent genes. Gene set z scores were compared between sample groups using Student *t* test. The top relatively upregulated and downregulated individual genes within each sample group (versus all other sample groups) were determined using fold change and Student *t* test. In case of quantitative proteomics data, tandem mass tag channel intensities of identified proteins were used for statistical analysis using Python 3.6.5. Channel intensities were $\log_2$ transformed and median normalized before applying independent Student *t*-test. *P* values were corrected for multiple hypotheses testing using Benjamini-Hochberg method. Differentially expressed proteins ($p<.05$) were analyzed using QIAGEN's Ingenuity Pathway Analysis software (IPA, QIAGEN Redwood City, CA, USA) to identify altered signaling pathways. The significance values (*P* value of overlap) for the canonical pathways were calculated by the right-tailed Fisher exact test. We used nonparametric rank-sum test to compare the groups because of the small number of cases per group. All statistical analyses were performed using JMP (SAS Institute, Cary, NC; version 14.1). *P* values less than .05 were considered to be statistically significant.

RESULTS

Clinical Characteristics

The demographics of the 17 COVID-19 autopsy cases are provided in Table 1. The cohort had a median age of 78 years (range, 29 to 94 years), and 14 (82.4%) were older than 70 years. There were 15 men, and 11 self-identified as White (64.7%). Three (17.6%) additional patients self-identified as Asian, none as Black. The time spent in the hospital varied widely, with 12 (70.6%) having been hospitalized for 5 or more days before death. Frequent and notable comorbidities included hypertension in 9 (52.9%), diabetes mellitus in 4 (23.5%), cardiovascular diseases (such as coronary artery disease) or cerebrovascular accident in 12 (70.6%), and chronic kidney disease in 1 (5.9%). Only 1 of 17 patients (5.9%) had no history of hypertension, diabetes mellitus, coronary artery disease, chronic kidney disease, or obesity. Seven (41.1%) were mechanically ventilated at the time of death.

All 17 patients who died with COVID-19 developed AKI. Among the patients with AKI who had a terminal serum creatinine level within 24 hours of death, eight had AKI stage 1 (47.1%), two had AKI stage 2 (11.8%), and three had AKI stage 3 (17.6%). One patient with AKI stage 3 received continuous renal replacement therapy. Urine dipstick assessment of proteinuria was unavailable in four patients, but in the remaining, all 13 patients (76.5%) had 100 mg/dL or less. Six of 17 patients had received treatment for COVID-19 including dexamethasone alone (n=1), remdesivir (n=1), a combination of dexamethasone and remdesivir (n=2), and a combination of remdesivir and convalescent plasma (n=2).

All 17 patients had a positive SARS-CoV-2 polymerase chain reaction, diagnosed at a median interval of 12 days before autopsy. At the time of autopsy, three (17.6%) were negative for SARS-CoV-2. The median postmortem interval was 18 hours and autolysis was only mild in 11 patients (64.7%). Sixteen (94.1%) died from complications of COVID-19 (all 16 had severe pulmonary disease, including acute bronchopneumonia superimposed on diffuse alveolar damage in eight [50.0%], acute and organizing pneumonia in four [25.0%], organizing pneumonia in three

TABLE 1. Cohort Demographics and Relevant Clinical Characteristics[a]

Characteristics	n (%)
Median age (range): 78 (29-94), years	
<50	1 (6)
50-70	2 (12)
70-90	12 (70)
>90	2 (12)
Male	15 (88)
Self-identified race	
Hispanic	0
Asian	3 (18)
Black	0
White	11 (64)
Unknown	3 (18)
Comorbidities	
Hypertension	9 (53)
Diabetes mellitus	4 (23)
Obesity	1 (6)
Cardiac disease (congestive heart failure/coronary artery disease)	10 (59)
Cerebrovascular accident	2 (12)
Cognitive decline	7 (41)
Chronic obstructive pulmonary disease	3 (18)
Cancer	3 (18)
Chronic kidney disease	1 (6)
None known	1 (6)
Duration of hospitalization, d	
Deceased on arrival	1 (6)
<1	4 (23)
5-10	5 (29)
10-15	2 (12)
15-20	2 (12)
>20	3 (18)
Mechanical ventilation	7 (41)
COVID-19 treatment	
Dexamethasone	1 (6)
Remdesvir	1 (6)
Remdesvir and dexamethasone	2 (12)
Remdesvir and convalescent plasma	2 (12)
Renal parameters	
AKI KDIGO stage	
1	8 (47)
2	2 (12)
3	3 (18)
Undetermined	4 (23)
Proteinuria, dipstick, mg	
<30	2 (12)
30-50	7 (41)
50-100	4 (23)
Unknown	4 (23)

[a]AKI, acute kidney injury; COVID-19, coronavirus disease 2019; KDIGO, Kidney Disease Improving Global Outcomes.

[18.8%], and diffuse alveolar damage alone in one [6.3%]).

Pathology Characteristics

The kidney autopsy findings are characterized in Table 2. Renal pathology was characterized by moderate-to-severe acute tubular injury in all (Figure 1A). Most showed marked simplification of the lining epithelium and luminal ectasia. Myoglobin casts were observed in two cases and osmotic tubulopathy in one. Tubulointerstitial inflammation was mild with macrophage and CD3-positive T-cell dominance. Peritubular capillaritis, with a mixed T-cell and macrophage immunophenotype was seen in 13 (76.5%) (Figure 1B-F). Similarly, glomerulitis, with a mixed T-cell and macrophage immunophenotype was seen in the same 13 (76.5%). The four patients who did not show microvascular inflammation had been treated with a combination of remdesivir and either dexamethasone (n=2) or convalescent plasma (n=2). Patients treated with dexamethasone alone or remdesivir alone had microvascular inflammation. Neutrophilic microvascular inflammation and interstitial infiltration was not a conspicuous feature in any of the cases. Nonimmune glomerular pathology included nodular diabetic glomerulosclerosis in 1 (5.9%); whereas collapsing focal segmental glomerulosclerosis or acute thrombotic microangiopathy was not identified. Marked peritubular capillary congestion was noted in all cases (Figure 1B and C). Moderate to severe arteriosclerosis and arteriolar hyalinosis were noted in 14 (82.4%) and 11 (64.7%), respectively. Only mild glomerulosclerosis (<25%) and tubulointerstitial scarring (<25%) were noted in all 17 autopsies.

The findings of microvascular inflammation suggested immune-mediated injury in severe COVID-19–associated renal disease. We further sought to characterize the molecular and ultrastructural profile of COVID-19 kidneys. Ultrastructural, transcriptomic, and proteomic profiles of the kidneys of seven patients who had only mild autolysis and

Mayo Clin Proc. ■ October 2021;96(10):2561-2575 ■ https://doi.org/10.1016/j.mayocp.2021.07.001
www.mayoclinicproceedings.org

for whom glutaraldehyde fixed tissue for ultrastructural examination was available were evaluated. The findings were compared with two age-matched non−COVID-19 control cohorts with AKI: S-AKI (all with bronchopneumonia) and NS-AKI. The clinical characteristics of the three groups are shown in Table 3. The mean age of the groups was 78, 71, and 74 years, respectively (P=.6). There were more women in the S-AKI group than in either of the other two groups. The mean terminal serum creatinine level was 3.0 mg/dL, 1.6 mg/dL, and 1.3 mg/dL, respectively (P=.32). All three groups had similar numbers of comorbidities and were comparable with respect to chronic microstructural changes in the renal parenchyma.

Morphological Characteristics of the Three AKI Cohorts

Microvascular inflammation (glomerulitis and peritubular capillaritis) was more prominent in patients with COVID-19 (5 of 7 patients) and S-AKI (7 of 7 patients), as compared with NS-AKI controls (0 of 7 patients). Mononuclear inflammatory cells were the predominant inflammatory cell type in both, whereas neutrophils were noted only infrequently, and only in S-AKI. Parenchymal tubulointerstitial inflammation was patchy, mild (3 of 7 patients), or moderate (4 of 7 patients), and largely mononuclear in COVID-19 and S-AKI, as compared with minimal inflammation in the NS-AKI controls (7 of 7 patients).

On ultrastructural evaluation of COVID-19 AKI, there was evidence of tubular injury with cytoplasmic vacuolization, loss of brush border, and mitochondrial injury. The latter was characterized by swelling, vacuolization, and distortion of cristae. Condensed mitochondria and distorted circular mitochondria were identified. Flocculent densities, and large vesicles with abundant clathrin-coated vesicles resembling viral particles were also identified (Figure 2A-C) Tubuloreticular inclusions were not seen in the

TABLE 2. Summary of Salient Autopsy Findings With Emphasis on Renal Pathology[a]

Autopsy characteristics	n (%)
SARS-CoV-2 polymerase chain reaction (n=17)	
Antemortem positivity	17 (100)
Duration from diagnosis to autopsy (median; range in days)	12 (0-67)
SARS-CoV-2 detected/indeterminate at autopsy	14 (82)
Median postmortem interval, hours	18
Cause of death (n=17)	
Complications of COVID-19	16 (94)
Ischemic heart disease	1 (6)
Pneumonia/diffuse alveolar damage (n=16)	
Acute bronchopneumonia	8 (50)
Acute and organizing bronchopneumonia	4 (25)
Organizing pneumonia	3 (19)
Diffuse alveolar damage	1 (6)
Extent of autolysis (n=17)	
Mild	11 (65)
Moderate	6 (35)
Severe	0 (0)
Renal pathology (n=17)	
Acute tubular injury	17 (100)
Glomerulitis, moderate	13 (76)
Dominant immunophenotype is mixed macrophage and T cell	13 (100)
Peritubular capillaritis, moderate	13 (76)
Dominant immunophenotype is mixed macrophage and T cell	13 (100)
Tubulointerstital inflammation	
Mild	17 (100)
Moderate	0 (0)
Severe	0 (0)
Immunophenotype	
Neutrophil	0 (0)
B cell	3 (18)
Mixed macrophage and T cell	17 (100)
Peritubular capillary congestion	17 (100)
Nonimmune glomerular pathology	
Nodular diabetic glomerulosclerosis	1 (6)
Acute thrombotic microangiopathy	0 (0)
Vascular pathology (n=17)	
Arteriolar hyalinosis, moderate to severe	11 (65)
Arterial sclerosis, moderate to severe	14 (82)
Interstitial fibrosis and tubular atrophy (n=17)	
Mild	17 (100)
Moderate	0 (0)
Severe	0 (0)

[a]COVID-19, coronavirus disease 2019; SARS-CoV-2, severe acute respiratory syndrome coronavirus 2.

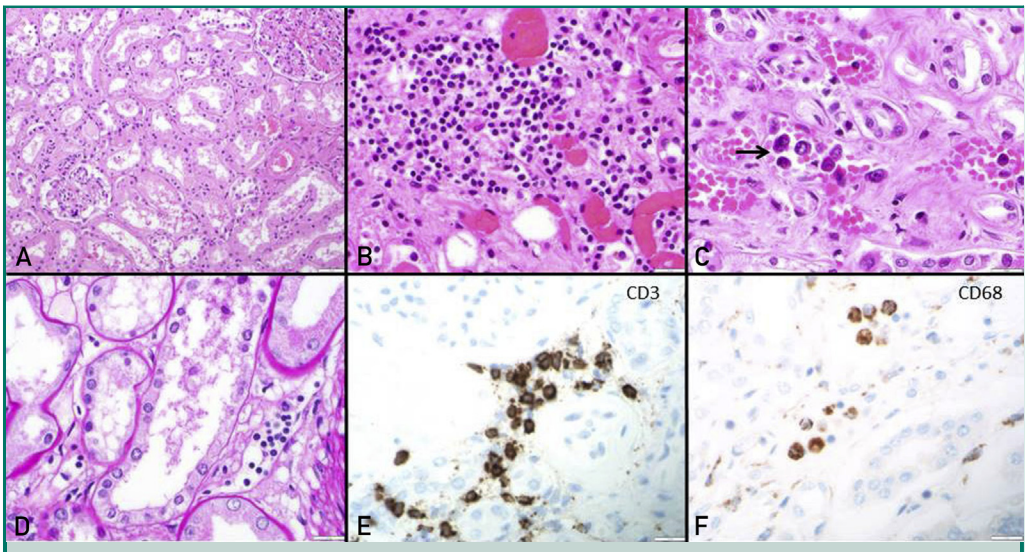

FIGURE 1. Acute tubular injury and immune cell infiltration in coronavirus disease 2019 kidneys. **(A)** The renal cortex on light microscopy shows acute tubular injury with lumina ectasia (hematoxylin and eosin [HE] stain, original magnification ×20). **(B)** Mild mononuclear interstitial infiltration and peritubular capillary congestion is noted (HE stain, original magnification ×40). (**C** and **D**) Peritubular capillaritis (**arrow**) is a notable feature within congested capillaries **(C)**. The microvascular inflammation is composed of CD3-positive T cells **(E)** and CD68-positive macrophages **(F)** (original magnification ×40 for E and F).

endothelial cytoplasm of COVID-19 cases. Peritubular capillary endothelial injury was noted. Multilayering of the glomerular and peritubular capillary basement membranes, features of more chronic endothelial injury, was not appreciated. Apoptosis of tubular epithelial cells was more common in COVID-19 (3.1/hpf) and S-AKI (4.1/hpf) as compared with NS-AKI controls (0.7/hpf) ($P<.001$) (Figure 2D-F).

SARS-CoV-2 IHC and in situ hybridization studies on kidney sections were negative in all seven COVID-19 cases. Definitive viral inclusions were not identified on ultrastructural studies of podocytes, endothelium, or tubules.

Molecular Characteristics of the Three AKI Cohorts

To define the phenotype of cellular infiltrates and the spatial architecture of AKI in COVID-19 kidneys, high-parameter imaging mass cytometry to detect 23 cell surface markers was performed on a Hyperion imaging system coupled to a Helios time-of-flight mass cytometer (Supplemental Table S1, available online at http://www.mayoclinicproceedings.org). Evidence of an adaptive immune response was suggested by the clustering of $CD3^+CD45RO^+$ cells in the tubulointerstitium in each case. The predominant innate immune response was underscored by an enriched population of macrophages ($CD68^+$) both in the interstitium and glomerular capillary loops (Figure 3A). The computational multiplex neighborhood analysis revealed that overall, the $CD3^+CD4^+$ cells were enriched in close proximity to antigen-presenting cells ($HLA\text{-}DR^+$), compared with $CD3^+CD4^-$ T cells and non−T cells (Figure 3B).

Kidney samples from COVID-19 cases and controls were analyzed by NanoString platform using the nCounter Human Organ Transplant Panel that profiles expression of 770 genes associated with different pathways related to immune response, tissue injury, and mechanisms of action for immunosuppressive drugs.[17]

Gene expression analysis revealed that COVID-19 kidneys had significant enrichment of multiple functional annotation transcript

Mayo Clin Proc. ■ October 2021;96(10):2561-2575 ■ https://doi.org/10.1016/j.mayocp.2021.07.001
www.mayoclinicproceedings.org

TABLE 3. Demographic and Relevant Clinicopathology Characteristics of Three Acute Kidney Injury Cohorts[a]

AKI cohort	Age, years/sex	Comorbidities	COVID-19/days from diagnosis/Rx	Serum creatinine (mg/dL)	AKI stage	Cause of AKI	ATN	Inflammation	TUNEL-positive (cells/hpf)	Capillary congestion	Chronicity	Other organ pathology
COVID-19												
1	71/M	HT, CAD	Positive/11/ Dexamethasone	7.19	3	COVID-19	+++	PTC-2 G-0 Interstitial	3	+++	Mild IFTA and GS	DAD, acute and organizing pneumonia
2	86/M	HT, CAD, CHF, dementia	Positive/6/none	6.28	3	COVID-19	+++	PTC-2 G-2 Interstitial	4	+++	Mild IFTA and GS	DAD, acute pneumonia
3	80/M	CVA, dementia, cancer	Positive/7/none	1.53	1	COVID-19	+++	PTC-2 G-2 Interstitial	3	+++	Mild IFTA and GS	DAD, acute pneumonia
4	73/M	DM, Cancer	Positive/ 25/ remdesvir + convalescent plasma	1.04	0	COVID-19	+++	PTC-0 G-0 Interstitial-0	2	+++	Mild IFTA and GS	DAD, organizing diffuse
5	93/M	Dementia, CHF, cancer	Positive/4/None	2.19	2	COVID-19	+++	PTC-2 G-2 Interstitial	3	+++	Mild IFTA and Mild GS	DAD, acute pneumonia
6	77/M	Dementia	Positive/12/None	0.79	1	COVID-19	+++	PTC-2 G-0 Interstitial	3	+++	Mild IFTA and GS	DAD, acute pneumonia
7	69/F	DM, CAD, HT, dementia	Positive/18/None	2.02	2	COVID-19	+++	PTC-0 G-0 Interstitial	4	+++	Mild IFTA and GS	DAD, acute pneumonia
Sepsis												
1	49/F	Obesity	Negative	1.41	1	E.coli sepsis with BP	+++	PTC–2 G-2 Interstitial	5	+	Mild IFTA and GS	Organizing and focal acute pneumonia
2	62/M	COPD; HT	Negative	1.6	1	E.coli sepsis with BP	+++	PTC-2 G-1 Interstitial	4	+	Mild IFTA and GS	Acute broncho pneumonia with DAD
3	62/M	Metastatic cancer; HT	Negative	1.76	1	Acute BP	+++	PTC-2 G-2 Interstitial	4	+	Mild IFTA and GS	Acute BP
4	85/F	HT/Carcinoma breast	Negative	1.2	1	Acute BP	+++	PTC-2 G-1 Interstitial	3	+	Mild IFTA and GS	Acute and organizing pneumonia with DAD

Continued on next page

TABLE 3. Continued

AKI cohort	Age, years/sex	Comorbidities	COVID-19/days from diagnosis/Rx	Serum creatinine (mg/dL)	AKI stage	Cause of AKI	ATN	Inflammation	TUNEL-positive (cells/hpf)	Capillary congestion	Chronicity	Other organ pathology
Sepsis, continued												
5	87/F	DM/HT/ Carcinoma lung	Negative	1.4	1	Acute BP	+++	PTC-2 G-1 Interstitial	3	+	Mild IFTA and GS	Squamous cell carcinoma lung
6	75/F	HT/ Heart failure	Negative	2.33	2	Acute BP	+++	PTC-2 G-1 Interstitial	6	+	Mild IFTA and GS	Gangrene bilateral toes and acute BP
7	78/M	HT/ Valvular heart disease	Negative	1.35	1	Acute BP	+++	PTC-1 G-1 Interstitial	4	+	Mild IFTA and GS	Acute and organizing pneumonia; Pulmonary microthrombi; splenic infarct
Non-sepsis												
1	84/M	HT, CAD, dementia	Negative	2.55	1	Hemodynamic	+++	PTC-0 G-1 Interstitial-0	1	_	Mild IFTA and GS	Atherosclerotic cardiovascular disease
2	81/F	CAD, CHF, HT	Negative	0.55	0	Hemodynamic	+++	PTC-0 G-1 Interstitial-0	0	_	Mild IFTA and GS	Ischemic heart disease
3	76/M	Dementia	Negative	1.7	1	Hemodynamic	+++	PTC-0 G-0 Interstitial-0	1	_	Mild IFTA and GS	Atherosclerotic cardiovascular disease
4	64/M	HT, DM, obesity	Negative	0.85	0	Hemodynamic	+++	PTC-0 G-0 Interstitial-0	0	_	Mild IFTA and GS	Atherosclerotic cardiovascular disease
5	66/M	CAD	Negative	1.9	1	Hemodynamic	+++	PTC-0 G-0 Interstitial-0	2	-	Mild IFTA and GS	Ischemic heart disease
6	78/M	HT	Negative	0.78	0	Hemodynamic	+++	PTC-0 G-0 Interstitial-0	1	-	Mild IFTA and GS	Atherosclerotic cardiovascular disease
7	70/M	CAD, HT, DM	Negative	0.9	0	Hemodynamic	+++	PTC-0 G-0 Interstitial-0	0	-	Mild IFTA and GS	Acute myocardial infarction

[a]AKI, acute kidney injury; ATN, acute tubular necrosis; BP, bronchopneumonia; CAD, coronary artery disease; CHF, congestive heart failure; COPD, chronic obstructive pulmonary disease; COVID-19, coronavirus disease 2019; CVA, cerebrovascular accident; DAD, diffuse alveolar damage; DM, diabetes; F, female; G, glomerulitis; GS, glomerulosclerosis; hpf, high power field; HT, hypertension; IFTA, interstitial fibrosis and tubular atrophy; M, male; PTC, peritubular capillary; Rx, treatment; TUNEL, terminal deoxynucleotidyl transferase of dUTP nick end labeling.

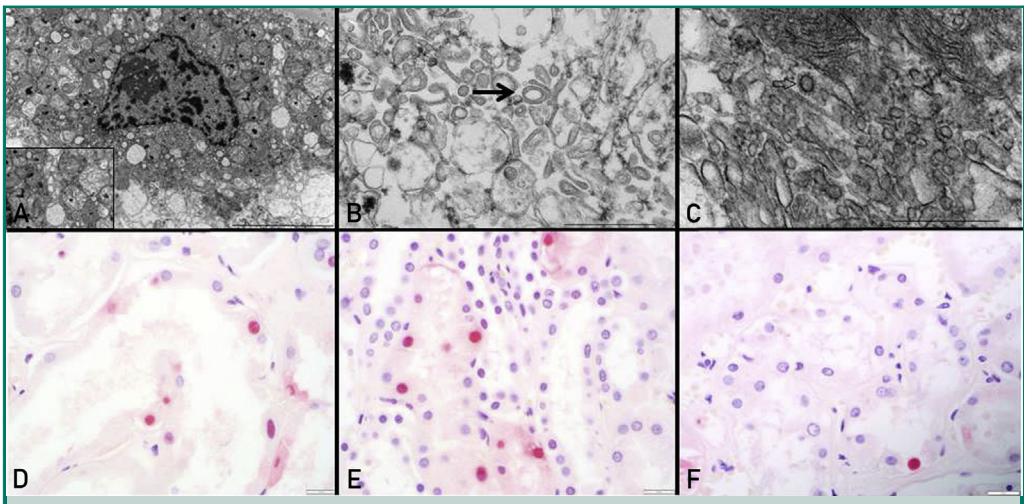

FIGURE 2. Evidence of tubular injury with mitochondrial insult and apoptosis in coronavirus disease 2019 kidneys. **(A)** Ultrastructural evaluation of proximal tubular epithelial cells show cytoplasmic vacuolization and swollen mitochondria with distorted cristae (see inset). **(B)** The mitochondrial injury includes ring- or donut-shaped mitochondria (**arrow**). **(C)** Clathrin-coated vesicles, easily mistaken for the virus, are also noted (**arrow**). Terminal deoxynucleotidyl transferase of dUTP (TUNEL) assay allows detection of TUNEL-positive cells (**black arrow**) in tubular epithelial cells of coronavirus disease 2019 kidneys **(D)**, sepsis-associated acute kidney injury **(E)**, and non-sepsis–related acute kidney injury **(F)**.

sets, including apoptosis, autophagy, major histocompatibility complex class I and II expression, and type 1 T helper cell and regulatory T cell (Treg) differentiation. The gene expression patterns of the COVID-19 cases resembled those of S-AKI (Figure 4).

In light of the inflammation observed in COVID-19 kidneys both morphologically and at the molecular level, we wanted to identify alterations in the proteome that could suggest unique mechanisms for COVID-19 AKI. Therefore, we performed quantitative proteomics analysis from formalin-fixed paraffin-embedded kidney sections of COVID-19 and both sets of control samples. A total of 3594 proteins were identified, of which 164 were differentially expressed between the groups ($P<.05$): 87 between COVID-19 and NS-AKI (16 with a fold-change $>$ 1.2), 81 between S-AKI and NS-AKI (8 with a fold-change $>$ 1.2), and 64 between COVID-19 and S-AKI (6 with a fold-change $>$ 1.2). A hierarchical clustering was conducted for all the proteins found in the three groups and a heat map was generated (Figure 5A). Ingenuity Pathway Analysis demonstrated that COVID-19 AKI kidneys were enriched in proteins involved in the sirtuin and necroptosis signaling pathways, both involved in regulatory response to inflammation (Supplemental Table S2, available online at http://www.mayoclinicproceedings.org). Ceramide signaling pathway upregulation was unique in COVID-19 kidneys when compared with NS-AKI, whereas oxidative phosphorylation was downregulated in COVID-19 AKI (Figure 5B).

DISCUSSION

Our study examined the morphologic and molecular characteristics of kidneys obtained during autopsies of patients who died of COVID-19. The morphological and molecular profile of severe COVID-19 renal injury resembles S-AKI.[19] This includes microvascular dysfunction with inflammation, that is, a macrophage-dominant cellular phenotype and a prominent T cell response in the tubulointerstitium in close proximity to antigen-presenting cells noted on spatial architectural analysis. The decreased oxidative phosphorylation and upregulation of ceramide-signaling pathways with ultrastructural evidence of mitochondrial injury

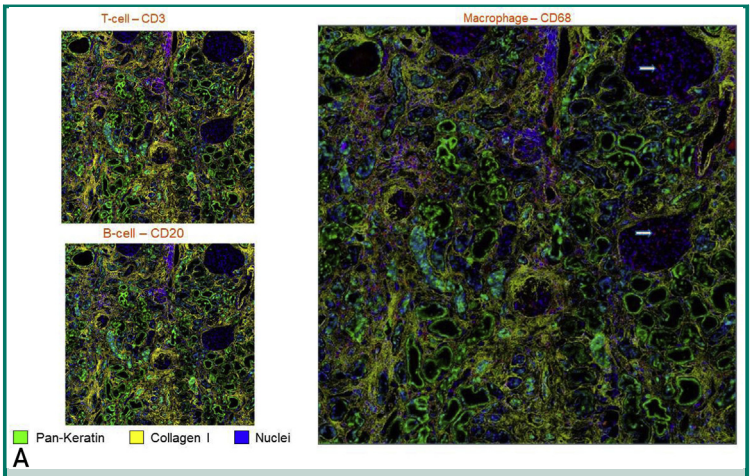

FIGURE 3. Hyperion imaging mass cytometry showing simultaneous immunophenotyping of inflammatory cells and renal structural components with exploration of their spatial relation. **(A)** Presence of T cells (**left, top**) and macrophages (**right**) in the tubulointerstitial compartment with a conspicuous absence of B cells (**left, bottom**). Glomerulitis is appreciated in the right panel with margination of macrophages (**arrows**). All cells of interest have been tagged red. **(B)** Computational image neighborhood analysis was performed after labeling tubules (PanK and E-cadherin), intertubular stroma (collagen and alpha smooth muscle actin) and glomeruli (vimentin) (**left**). After cells were classified using a supervised approach ($CD4^+$ T cells, $CD4^-$ T cells, and non-T cells), a distance map measuring the closest distance from the HLA-DR+ cells to each of the other cells was generated (middle, HLA-DR in yellow, distance from HLA-DR shown in increasing intensity of blue color). The percent of cells within each defined distance bin is displayed (right).

noted in COVID-19 AKI indicates metabolic reprogramming of tubular epithelial cells that has been described in S-AKI.

COVID-19—Associated Inflammatory Response

Overall, the COVID-19 kidneys had significantly more inflammation compared with NS-AKI controls. The molecular signals of inflammation and immune activation observed in COVID-19 kidneys suggests a global antiviral response characterized by a macrophage and T-cell—rich inflammation, and type II interferon production, as widely suggested by blood-based assays.[20,21] The $CD4^+$-dominant T-cell response, as we observed in the COVID-19 kidneys, has been associated with worse clinical outcomes.[22] Severe acute respiratory syndrome coronavirus 2—specific $CD4^+$ T cells directed to the spike surface glycoprotein have been detected in patients with severe COVID-19, and may account for the $CD4^+$ T cells found in the tubulointerstitial compartment of the kidneys.[23] The molecular pathways, investigated both at the genomic and proteomic level, confirmed that inflammation is the predominant driver of the renal injury seen in COVID-19, similar to S-AKI. In both groups, we found increased expression of gene sets associated with counter regulatory mechanisms normally seen in immune activation, including Treg differentiation and sirtuin signaling.[24] In severe COVID-19 cases, increase in circulating Treg frequency is associated with worse outcomes, presumed secondary to suppression of antiviral T-cell responses.[25]

COVID-19—Associated Signaling Pathways

In COVID-19 kidneys, as well as in S-AKI, we found evidence of increased apoptosis. Although apoptosis is potentially virally mediated via the extrinsic pathways,[26] the upregulated ceramide pathway noted in our COVID-19 AKI cohort coupled with the reduced oxidative phosphorylation signals suggest that ceramide-induced apoptosis via mitochondrial disruption might play a role in tubular cell death.[27] Mitochondria of the proximal tubular epithelial cells of the COVID-19 kidneys showed marked vacuolization and distortion of the cristae as has been described previously.[28] The upregulated ceramide pathway in COVID-19 AKI underscores the role of lipid dysregulation in severe COVID-19 as suggested by others.[29] Necroptosis, an immunogenic cell death pathway that can eliminate virus-infected cells and mobilize both innate and adaptive immune responses to restrict virus replication, was also more profound in COVID-19 kidneys, compared with NS-AKI. Necroptosis plays a major role in lung injury following SARS-COV2 infection.[26,30,31]

COVID-19 AKI Resembles Sepsis-Associated AKI

Kellum et al[16] and others have suggested that COVID-19 AKI is very similar to S-AKI.[32] Our observations of microvascular dysfunction,

Mayo Clin Proc. ■ October 2021;96(10):2561-2575 ■ https://doi.org/10.1016/j.mayocp.2021.07.001
www.mayoclinicproceedings.org

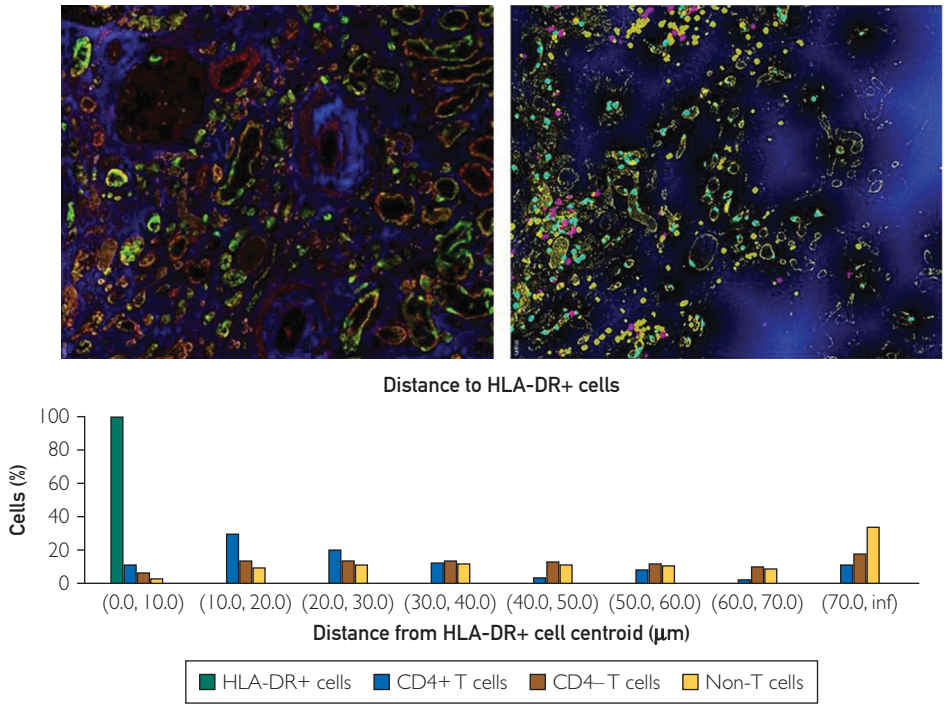

FIGURE 3. Continued

inflammation, and the metabolic reprogramming (decreased oxidative phosphorylation and increased ceramide signaling) in COVID-19 AKI are similar to the fundamental pathophysiologic mechanisms described in S-AKI.[19,33,34] We summarize the key findings in our study and draw comparisons to published literature in COVID-AKI and S-AKI in Table 4.[19,26,29,31,33-38] These pathologies show potential therapeutic targets for COVID-19.

Study Limitations

The main limitation of the current study is that although we had the ability to compare molecular characteristics of COVID-19–related pathology against S-AKI autopsies, we were not able to compare with autopsies of patients who died of other viral-mediated AKI. This requires planning and prospective studies to obtain optimal preservation of autopsy tissue for omics studies. The preservation artifacts noted on ultrastructural studies of archived formalin-fixed non–COVID-19 autopsy tissue from prior patients did not allow for comparison. Additionally, statistical analysis did not adjust for multiple testing and a larger sample size could have provided a more robust gene expression analysis. The strength of our study is that we were able to perform a detailed morphological analysis and multi-omic platform approach to study severe COVID-19 kidney injury and draw parallels to sepsis-associated injury.

CONCLUSION

This series is dedicated to the renal histopathologic, ultrastructural, and molecular findings in patients who had SARS-CoV-2 infection, which provides evidence for an innate and prominent T cell immune response. The morphological and molecular characteristics of COVID-19

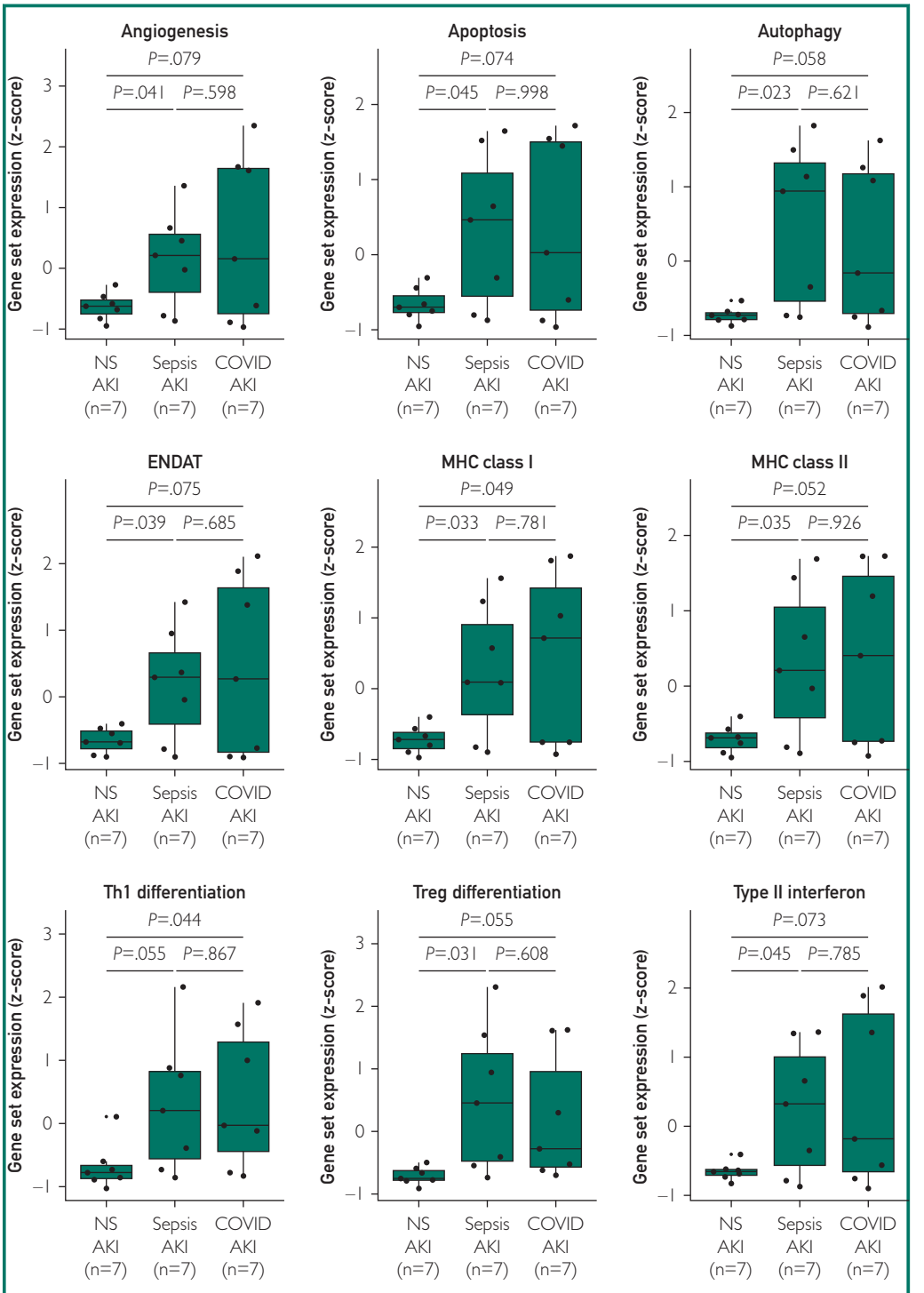

FIGURE 4. Transcriptomic analysis. Box plots show the relative expression of select functional annotation gene sets between coronavirus disease 2019 (COVID-19) acute kidney injury (AKI), sepsis-related AKI (S-AKI) and nonsepsis-related AKI (NS-AKI). ENDAT, endothelial cell-associated transcripts; MHC, major histocompatibility complex; Th1, type 1 T helper cell; Treg, regulatory T cell.

Mayo Clin Proc. ■ October 2021;96(10):2561-2575 ■ https://doi.org/10.1016/j.mayocp.2021.07.001
www.mayoclinicproceedings.org

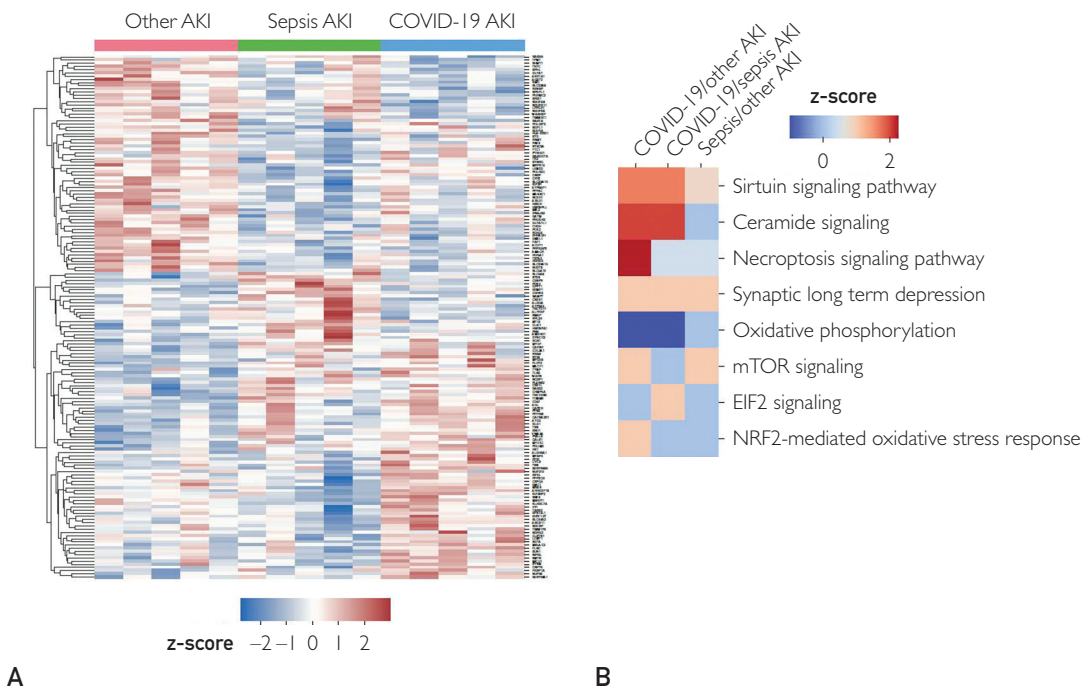

FIGURE 5. Proteomic analysis. **(A)** The heat map gives a global overview of the differential expression of protein levels for each individual gene in the three acute kidney injury (AKI) cohorts. Proteins that were significantly over- (**red**) or under-expressed (**blue**) at $P<.05$ are shown. **(B)** The Ingenuity Pathway Analysis of differential protein expression in coronavirus disease 2019 (COVID-19) AKI, sepsis-associated AKI, and other AKI controls is shown. EIF2, Eukaryotic initiation factor 2; mTOR, mammalian target of rapamycin; NRF2, nuclear factor erythroid 2–related factor 2.

AKI resemble those of S-AKI. Mitochondrial dysfunction may play a central role in COVID-19 AKI.

ACKNOWLEDGMENT

Drs Badley, Pandey, and Taner contributed equally to this work. Ms Katie Reed and

TABLE 4. Morphological and Molecular Comparison of COVID-19 AKI to Sepsis AKI[a]

	COVID- 19	Sepsis	References[b]
Morphology			
Immune response and microvascular inflammation	++	++	19,33,34
Apoptosis	+	+	26
Molecular			
Gene expression analysis			
Apoptosis, autophagy, MHC class I and II expression, Th1 Treg differentiation	+	++	
Proteomic pathway analysis			
Sirtuin signaling pathway	++	+	35,36
mTOR signaling pathway	+	+	37
Necroptosis	++	+	26,30,31
Oxidative phosphorylation	–		38
Ceramide signaling pathway	++		29

[a]COVID-19, coronavirus disease 2019; MHC, major histocompatibility complex; mTOR, mammalian target of rapamycin; Th1, type 1 T helper cell; Treg, regulatory T cell.
[b]Several studies were used to form this comparison set.[19,26,29-31,33-38]

Tiffany Mainella provided research for support.

SUPPLEMENTAL ONLINE MATERIAL

Supplemental material can be found online at http://www.mayoclinicproceedings.org. Supplemental material attached to journal articles has not been edited, and the authors take responsibility for the accuracy of all data.

Potential Competing Interests: The authors report no potential competing interests.

Grant Support: Research funding was obtained from the Anatomic Pathology Research Funds, Department of Laboratory Medicine and Pathology, Mayo Clinic.

Correspondence: Address to Mariam P. Alexander, MD, Department of Laboratory Medicine and Pathology, Mayo Clinic, 200 First Street SW, Rochester, MN 55905, USA (alexander.mariam@mayo.edu; Twitter: @MPAlexanderMD).

ORCID

Mariam P. Alexander: https://orcid.org/0000-0001-9072-9871; Kiran K. Mangalaparthi: https://orcid.org/0000-0002-5791-727X; Anil K. Madugundu: https://orcid.org/0000-0003-4274-7316; Ann M. Moyer: https://orcid.org/0000-0003-2590-7218; Benjamin A. Adam: https://orcid.org/0000-0003-1908-1739; Michael Mengel: https://orcid.org/0000-0002-7222-3356; Sandra M. Herrmann: https://orcid.org/0000-0002-3700-4537; Rondell P. Graham: https://orcid.org/0000-0002-8686-4867; Denic Aleksandar: https://orcid.org/0000-0001-9157-5405; Reade A. Quinton: https://orcid.org/0000-0002-3231-8078; Peter T. Lin: https://orcid.org/0000-0003-3012-4728; Kevin D. Pavelko: https://orcid.org/0000-0001-7555-1315; Ramya Narasimhan: https://orcid.org/0000-0002-3310-1364; Trevor D. McKee: https://orcid.org/0000-0002-2195-6146; Akhilesh Pandey: https://orcid.org/0000-0001-9943-6127

REFERENCES

1. Hirsch JS, Ng JH, Ross DW, et al. Acute kidney injury in patients hospitalized with COVID-19. *Kidney Int*. 2020;98(1):209-218.
2. Pei G, Zhang Z, Peng J, et al. Renal involvement and early prognosis in patients with COVID-19 pneumonia. *J Am Soc Nephrol*. 2020;31(6):1157-1165.
3. Cheng Y, Luo R, Wang K, et al. Kidney disease is associated with in-hospital death of patients with COVID-19. *Kidney Int*. 2020;97(5):829-838.
4. Kudose S, Batal I, Santoriello D, et al. Kidney biopsy findings in patients with COVID-19. *J Am Soc Nephrol*. 2020;31(9):1959-1968.
5. Su H, Yang M, Wan C, et al. Renal histopathological analysis of 26 postmortem findings of patients with COVID-19 in China. *Kidney Int*. 2020;98(1):219-227.
6. Santoriello D, Khairallah P, Bomback AS, et al. Postmortem kidney pathology findings in patients with COVID-19. *J Am Soc Nephrol*. 2020;31(9):2158-2167.
7. Bois MC, Boire NA, Layman AJ, et al. COVID-19—associated nonocclusive fibrin microthrombi in the heart. *Circulation*. 2021;143(3):230-243.
8. Basso C, Leone O, Rizzo S, et al. Pathological features of COVID-19—associated myocardial injury: a multicentre cardiovascular pathology study. *Eur Heart J*. 2020;41(39):3827-3835.
9. Roden AC, Bois MC, Johnson TF, et al. The spectrum of histopathologic findings in lungs of patients with fatal coronavirus disease 2019 (COVID-19) infection. *Arch Pathol Lab Med*. 2021;145(1):11-21.
10. Carsana L, Sonzogni A, Nasr A, et al. Pulmonary post-mortem findings in a series of COVID-19 cases from northern Italy: a two-centre descriptive study. *Lancet Infect Dis*. 2020;20(10):1135-1140.
11. Hanley B, Naresh KN, Roufosse C, et al. Histopathological findings and viral tropism in UK patients with severe fatal COVID-19: a post-mortem study. *Lancet Microbe*. 2020;1(6):e245-e253.
12. Menter T, Haslbauer JD, Nienhold R, et al. Postmortem examination of COVID-19 patients reveals diffuse alveolar damage with severe capillary congestion and variegated findings in lungs and other organs suggesting vascular dysfunction. *Histopathology*. 2020;77(2):198-209.
13. Puelles VG, Lutgehetmann M, Lindenmeyer MT, et al. Multiorgan and renal tropism of SARS-CoV-2. *N Engl J Med*. 2020;383(6):590-592.
14. Stasi A, Castellano G, Ranieri E, et al. SARS-CoV-2 and viral sepsis: immune dysfunction and implications in kidney failure. *J Clin Med*. 2020;9(12):4057.
15. Golmai P, Larsen CP, DeVita MV, et al. Histopathologic and ultrastructural findings in postmortem kidney biopsy material in 12 patients with AKI and COVID-19. *J Am Soc Nephrol*. 2020;31(9):1944-1947.
16. Kellum JA, Nadim MK, Forni LG. Sepsis-associated acute kidney injury: is COVID-19 different? *Kidney Int*. 2020;98(6):1370-1372.
17. nCounter Human Organ Transplant Panel. https://www.nanostring.com/products/ncounter-assays-panels/immunology/human-organ-transplant/. Accessed June 1, 2021.
18. Adam B, Afzali B, Dominy KM, et al. Multiplexed color-coded probe-based gene expression assessment for clinical molecular diagnostics in formalin-fixed paraffin-embedded human renal allograft tissue. *Clin Transplant*. 2016;30(3):295-305.
19. Gomez H, Kellum JA. Sepsis-induced acute kidney injury. *Curr Opin Crit Care*. 2016;22(6):546-553.
20. de Candia P, Prattichizzo F, Garavelli S, Matarese G. T cells: warriors of SARS-CoV-2 infection. *Trends Immunol*. 2021;42(1):18-30.
21. Sattler A, Angermair S, Stockmann H, et al. SARS-CoV-2—specific T cell responses and correlations with COVID-19 patient predisposition. *J Clin Invest*. 2020;130(12):6477-6489.
22. Mathew D, Giles JR, Baxter AE, et al. Deep immune profiling of COVID-19 patients reveals distinct immunotypes with therapeutic implications. *Science*. 2020;369(6508):eabc8511.
23. Weiskopf D, Schmitz KS, Raadsen MP, et al. Phenotype and kinetics of SARS-CoV-2-specific T cells in COVID-19 patients with acute respiratory distress syndrome. *Sci Immunol*. 2020;5(48):eabd2071.
24. Mendes KL, Lelis DF, Santos SHS. Nuclear sirtuins and inflammatory signaling pathways. *Cytokine Growth Factor Rev*. 2017;38:98-105.
25. Galvan-Pena S, Leon J, Chowdhary K, et al. Profound Treg perturbations correlate with COVID-19 severity. *bioRxiv*. 2020.
26. Li S, Zhang Y, Guan Z, et al. SARS-CoV-2 triggers inflammatory responses and cell death through caspase-8 activation. *Signal Transduct Target Ther*. 2020;5(1):235.
27. Ueda N. Ceramide-induced apoptosis in renal tubular cells: a role of mitochondria and sphingosine-1-phoshate. *Int J Mol Sci*. 2015;16(3):5076-5124.
28. Papadimitriou JC, Drachenberg CB, Kleiner D, Choudhri N, Hanirian A, Cebotaru V. Tubular epithelial and peritubular

capillary endothelial injury in COVID-19 AKI. *Kidney Int Rep*. 2021;6(2):518-525.
29. Caterino M, Gelzo M, Sol S, et al. Dysregulation of lipid metabolism and pathological inflammation in patients with COVID-19. *Sci Rep*. 2021;11(1):2941.
30. Nailwal H, Chan FK. Necroptosis in anti-viral inflammation. *Cell Death Differ*. 2019;26(1):4-13.
31. Galluzzi L, Kepp O, Chan FK, Kroemer G. Necroptosis: mechanisms and relevance to disease. *Annu Rev Pathol*. 2017;12:103-130.
32. Olwal CO, Nganyewo NN, Tapela K, et al. Parallels in Sepsis and COVID-19 Conditions: Implications for Managing Severe COVID-19. *Front Immunol*. 2021;12:602848.
33. Lerolle N, Nochy D, Guerot E, et al. Histopathology of septic shock induced acute kidney injury: apoptosis and leukocytic infiltration. *Intensive Care Med*. 2010;36(3):471-478.
34. Zarjou A, Agarwal A. Sepsis and acute kidney injury. *J Am Soc Nephrol*. 2011;22(6):999-1006.
35. Miller R, Wentzel AR, Richards GA. COVID-19: NAD(+) deficiency may predispose the aged, obese and type2 diabetics to mortality through its effect on SIRT1 activity. *Med Hypotheses*. 2020;144:110044.
36. Li L, Chen Z, Fu W, Cai S, Zeng Z. Emerging evidence concerning the role of sirtuins in sepsis. *Crit Care Res Pract*. 2018;2018:5489571.
37. Cheng Mm W, Long Y, Wang H, Han Mm W, Zhang J, Cui N. Role of the mTOR Signalling Pathway in Human Sepsis-Induced Myocardial Dysfunction. *Can J Cardiol*. 2019;35(7):875-883.
38. Shenoy S. Coronavirus (COVID-19) sepsis: revisiting mitochondrial dysfunction in pathogenesis, aging, inflammation, and mortality. *Inflamm Res*. 2020;69(11):1077-1085.